^{27}Al NMR in grain-aligned ternary intermetallic $CeNi_2Al_5$: A dense Kondo compound

R. Sarkar, K. Ghoshray, B. Bandyopadhyay, and A. Ghoshray*
Experimental Condensed Matter Physics Division, Saha Institute of Nuclear Physics, 1/AF Bidhannagar, Kolkata 700064, India
(Received 15 November 2004; published 28 March 2005)

We report ^{27}Al NMR studies of $CeNi_2Al_5$ and $LaNi_2Al_5$ in 7 T and in the range 3.5–300 K. $CeNi_2Al_5$ is dense Kondo compound that orders antiferromagnetically at 2.6 K. For two inequivalent Al sites for the Ce compound, the nuclear quadrupolar splitting frequency, ν_Q is 0.98 and 2.52 MHz, respectively. Knight shifts for both the sites are almost equal in magnitude and follow a linear relation with molar susceptibility in the range 30–300 K. The transferred hyperfine coupling constant, $H_{hf}=1.84$ kOe/μ_B, is small compared to those in other Ce compounds. The behavior of $1/T_{1f}$ for the two Al sites is widely different. For the Al(1) site, with one nearest-neighbor Ce ion, the $4f$-electron spin-fluctuation process dominates over the Korringa contribution. In particular, the Ce-$4f$ spin correlation nearest to Al(1) starts to develop below 150 K. Finally near 12 K, the fluctuation frequency of the $4f$ spin becomes comparable to the ^{27}Al NMR frequency, resulting in the reduction of $1/T_{1f}$ with further lowering of temperature. For the Al(2) site, which sits in between two Ce near neighbors, the relaxation process is dominated by the Korringa contribution in the range 12–300 K. It could, however, sense the effect of $4f$ spin correlations below 12 K. The widely different ^{27}Al nuclear relaxation mechanisms for two inequivalent Al sites in the unit cell of $CeNi_2Al_5$ indicate that the effect of the spin fluctuation due to the Kondo effect overcomes that due to the Rudderman-Kittel-Kasuya-Yosida interaction for the Al(2) site in the range 12–300 K. On the other hand, the behavior of $1/T_{1f}$ for the Al(1) site resembles that of $CeAl_2$.

DOI: 10.1103/PhysRevB.71.104421 PACS number(s): 76.60.−k

I. INTRODUCTION

Dense Kondo compounds have revealed complicated and fascinating magnetic properties due to the competition between Kondo and Rudderman-Kittel-Kasuya-Yosida (RKKY) interactions. In the past, many cerium compounds showing such a competition have been investigated. Members in the ternary Ce-Ni-Al system[1] are no exception. Among all the different phases in this phase, the Al-rich portion of the intermetallics[2] has attracted much attention due to its exceptional electronic and magnetic properties. For example, $CeNiAl_4$ is nonmagnetic down to 1.6 K, with the resistivity behavior resembling a dense Kondo system[3,4] with Kondo temperature $T_K \sim 60$ K. Moreover, the ^{27}Al NMR showed a signature in the s-f hybridization below T_K.[5,6] On the other hand, $CeNi_2Al_5$ is an antiferromagnetic (AF) dense Kondo compound with $T_N=2.6$ K.[7] The temperature dependence of the resistivity shows a broad minimum around 30 K; a $-\ln T$ behavior appears down to 5 K and drops abruptly at 2.6 K after a broad maximum around 4 K. This was defined as the Kondo temperature T_K. The magnetic transition has been confirmed by resistivity, magnetic susceptibility, and specific heat measurements. The orthorhombic local symmetry leads to a strong crystal-electric-field (CEF) effect, and a very large anisotropy was observed. The consequence of a comparable T_N and T_K indicates a complex relation between the Kondo effect, the RKKY interaction and the CEF effect in $CeNi_2Al_5$. A neutron diffraction measurement[8] on the single crystal at 1.4 K indicated that the magnetic structure is sine-wave modulated with a propagation vector $\mathbf{k}=(1/2,2/5,1/12)$. The maximum amplitude of the magnetic moment is equal to 1.54 μ_B and its direction is tilted 8° from the b axis toward the a axis. Precise determination of the magnetic structure was done by Givord *et al.*[9] A more recent magnetization measurement at 400 mK and magnetostriction at 1.2 K (Ref. 10) lead the authors to contend that not only the Kondo effect but also the magnetoelastic and/or quadrupolar effects should be taken into account to explain the system. A very recent electronic structure calculation[2] reveals that the Al-rich compounds in the Ce-Ni-Al system may be considered as "polar intermetallics" because the Fermi level coincides with the separation of bonding and antibonding states of the Ni-Al framework. Thus a complex nature of the electronic structure demands further study.

There had been only one publication involving NMR and nuclear quadrupole resonance (NQR) studies[11] of ^{27}Al in the powder sample of $CeNi_2Al_5$ and the focus was on the AF-ordered state by NQR. However, the authors could not shed much light on the paramagnetic state because of the overlapping of the quadrupole-split NMR lines from different Al sites with unequal values of the quadrupole frequencies $\nu_Q = 3e^2qQ/20h$. The broad NQR spectra below T_N suggested the presence of a complicated spin structure with spiral or sinusoidal modulation. In this paper we have reported detailed ^{27}Al NMR studies in a grain-aligned sample of $CeNi_2Al_5$ in the temperature range 3.5–295 K. A very large anisotropy in the magnetic susceptibility[8] facilitates the alignment of the polycrystalline sample in the presence of a magnetic field along the b axis. Thus the grain-aligned sample allows us to observe clearly resolved satellite transitions and consequently the site assignment is unique. Therefore, the Knight shift and the nuclear spin-lattice relaxation rate $(1/T_1)$ could be determined with sufficient accuracy. We have taken $LaNi_2Al_5$ as a reference material, as it has the same crystal structure as $CeNi_2Al_5$, with very close lattice parameters and, apart from the Ce $4f$ electrons, similar electronic configurations are expected for both compounds.[12,13]

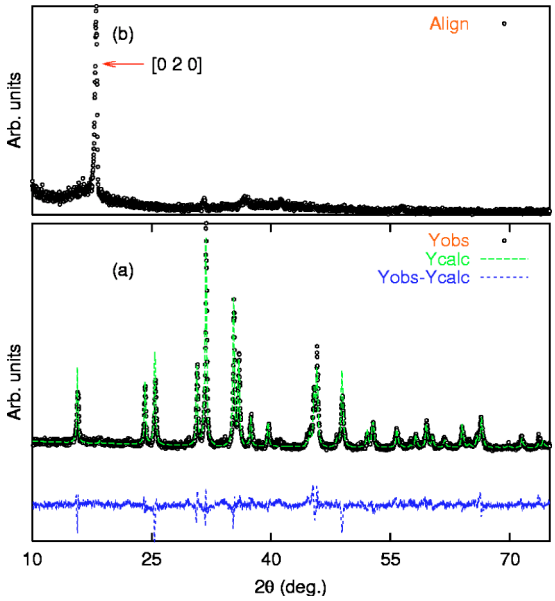

FIG. 1. (Color online) Typical XRD spectra of $CeNi_2Al_5$ in (a) random powder and (b) grain-oriented powder obtained as mentioned in the text.

II. EXPERIMENTAL

A. Sample preparation and characterization

The polycrystalline samples of $CeNi_2Al_5$ and $LaNi_2Al_5$ were prepared by repeated arc melting of the stoichiometric amounts of the constituent elements of high purity in an Ar-arc furnace. We then annealed the ingot wrapped in the tantalum foil at 1000 °C under vacuum for 7 days to minimize the defects. The x-ray diffraction (XRD) pattern of the powder sample of $CeNi_2Al_5$, as shown in Fig. 1(a), confirms the single-phase nature of the compound. The cell parameters refined by the Rietveld method using the FULLPROF program[14] agree very well with orthorhombic $PrNi_2Al_5$-type structure (space group *Immm*), with lattice parameters[1] $a=7.021$ Å, $b=9.604$ Å, $c=3.991$ Å. Another part of the finely powdered sample was then mixed with the low viscosity and low magnetic susceptibility epoxy (EPOTEK 301) in a cylindrical quartz tube and placed in a magnetic field of 7.04 T for 48 h for NMR measurement. A flat sample was also prepared for XRD studies to test whether the *b* axis of the grain-aligned sample was perpendicular to the surface of the plate. XRD patterns for an aligned sample [Fig. 1(b)] and that of the random powder of $CeNi_2Al_5$ suggest that the majority of the grains in the aligned powder have their *b* axis parallel to each other. In the case of $LaNi_2Al_5$, we were able to orient the crystallites partially but, most importantly, the *b* axis of the crystallites, as in $CeNi_2Al_5$, were oriented along the magnetic field. The crystal structure is drawn in Fig. 2. In the unit cell there are two inequivalent Al sites, denoted here as Al(1) and Al(2). The Al(1) site has a *mm* site symmetry having a multiplicity of 8. The Al(2) site has a site symmetry of *mmm* with a multiplicity of 2.

B. NMR measurement

^{27}Al NMR experiments were performed in a Bruker MSL 100 spectrometer with a 7.04 T superconducting magnet.

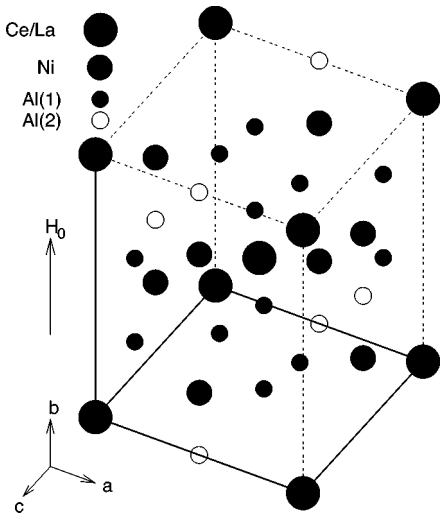

FIG. 2. Crystallographic unit cell of $(Ce/La)Ni_2Al_5$ along the *b* axis. The big arrow shows the direction of the magnetic field applied to orient the crystallites.

The direction of the applied field was always kept parallel to the *b* axis in the case of the oriented sample. Temperature variation was performed in an Oxford cryostat with an ITC 503 temperature controller in the range 3.5–295 K. The spectrum was recorded by applying a $\pi/2-\tau-\pi/2$ solid echo sequence. Knight shifts were measured with respect to the reference position (ν_R) of ^{27}Al resonance in a $AlCl_3$ solution. At high temperature, the spectra, at a fixed magnetic field, were obtained by exciting, at a large frequency range, a broad part of the spectrum, and recording in each step, the amplitude of the Fourier-transformed spin-echo signal. Below 20 K, where the lines broaden, the spectra were obtained by exciting, at small frequency steps, a narrow part of the spectrum, and recording in each step the amplitude of the Fourier-transformed spin-echo signal.

III. TRANSFERRED HYPERFINE INTERACTION AND NMR SPECTRA

In a system such as $CeNi_2Al_5$, the Hamiltonian for a ^{27}Al nucleus with spin $I=5/2$ in the presence of a magnetic field H_0 is written as $H=H_0+H_{cond}+H_M+H_Q$, where H_0 is the Zeeman term, H_{cond} represents the magnetic coupling between the conduction electron spin and the nuclear spin, and is temperature independent. The term H_M arises due to the interaction of the *f* electrons with the probed nuclei, via the conduction electrons, and is temperature dependent. However, in case of $LaNi_2Al_5$, the term H_M does not arise. H_Q is the electric quadrupole interaction. Assuming that the principal axes of the electric-field-gradient (EFG) tensor and the magnetic shift tensor are coincident, the resonance frequency ν of a given transition $(m \leftrightarrow m-1)$ is given by

$$\nu(m \leftrightarrow m-1) = \nu_0 + \nu_{quad}^{(1)} + \nu_{quad}^{(2)} + \nu_{ani}. \quad (1)$$

Details can be seen, for example, in Ref. 15.

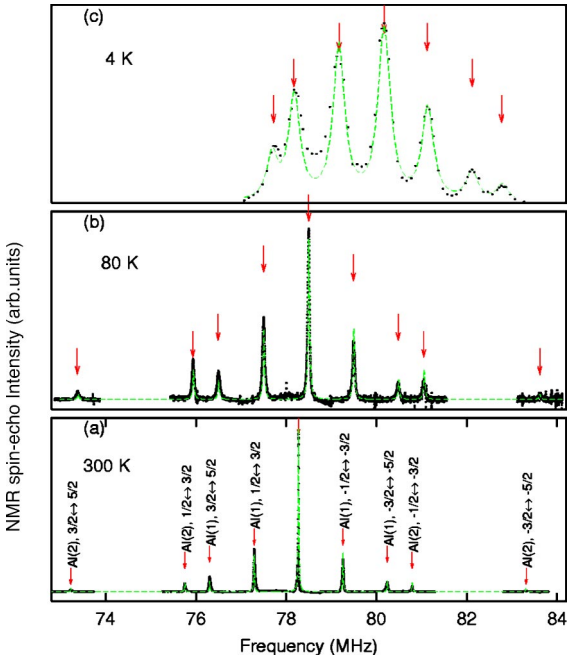

FIG. 3. (Color online) Some typical ^{27}Al NMR spectra of $CeNi_2Al_5$ at 7.04 T at different temperatures. The dashed line indicates the theoretically fitted spectrum. (a) Different transitions for Al(1) and Al(2) sites are shown. The central transitions for both the sites coincide. (b) and (c) The arrows (↓) indicate the corresponding transitions same as 300 K. (c) $\pm 3/2 \leftrightarrow \pm 5/2$ transitions for Al(2) are not shown.

A. ^{27}Al NMR in $CeNi_2Al_5$

Figure 3 shows the ^{27}Al NMR spectra of $CeNi_2Al_5$ at different temperatures. The central transitions for Al(1) and Al(2) sites merge with each other; however, clearly resolved two pairs of satellite transitions for these two sites were observed. Considering the intensity of each line and the multiplicity of each Al site in the unit cell as seen in Fig. 2, we have assigned the two innermost pairs to the Al(1) site; the outermost two pairs arise because of Al(2). Observation of the overlapped central transitions suggest that the Knight shift for the two types of Al sites are close to each other. However, clearly resolved satellite transitions indicate a significant difference in the quadrupolar interaction parameters between the two Al sites. On lowering the temperature the spectra shift continuously towards the high-frequency side with a gradual line broadening, which has been considerably enhanced below 10 K such that the satellite lines for the different Al sites start to superimpose partially. For example, Fig. 4 shows only the $-1/2 \leftrightarrow -3/2$ transition for the Al(1) site in the temperature range 3.6–8 K. Thus it was always possible to measure the shift and $1/T_1$ by exciting only the desirable single resonance line with accuracy. Therefore the shift and the quadrupolar interaction parameters throughout the whole temperature range are determined by fitting the experimental spectra using Eq. (1). The ν_Q for the Al(1) and Al(2) sites are found to be 0.984 and 2.520 MHz with $\eta = 0.3$ and 0.075, respectively. These values are very close to those reported by Fujiwara *et al.*[11] Quadrupolar interaction parameters remain almost unaltered down to 3.5 K, indicating the absence of any structural change in the range 3.5–300 K.

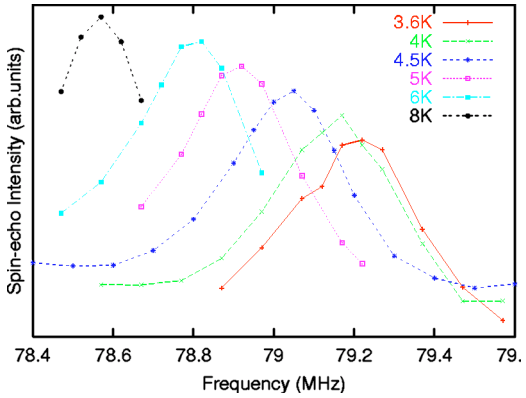

FIG. 4. (Color online) Temperature dependence of the $-1/2 \leftrightarrow -3/2$ transition for the Al(1) site of $CeNi_2Al_5$.

B. ^{27}Al NMR in $LaNi_2Al_5$

Figure 5(a) shows the ^{27}Al NMR spectra of the oriented sample of $LaNi_2Al_5$ at 300 K. Exactly similar spectra with the same amount of shift were observed down to 80 K. Structure around the central line arises because of the imperfect orientation. As in $CeNi_2Al_5$, we have assigned the two inner pairs of lines as due to the Al(1) site. We could detect only the $\pm 3/2 \leftrightarrow \pm 1/2$ transition for the Al(2) site. Other transitions could not be detected at any temperature. This may be a fact of the imperfect alignment causing line broadening. ν_Q and η values for both the Al(1) and Al(2) sites are found to close as in $CeNi_2Al_5$. Figure 5(b) shows the NMR spectrum due to randomly oriented powder. Structure around the central line [shown more clearly in the inset of Fig. 5(b)] reveals the characteristics points ν_H and ν_L of the second-

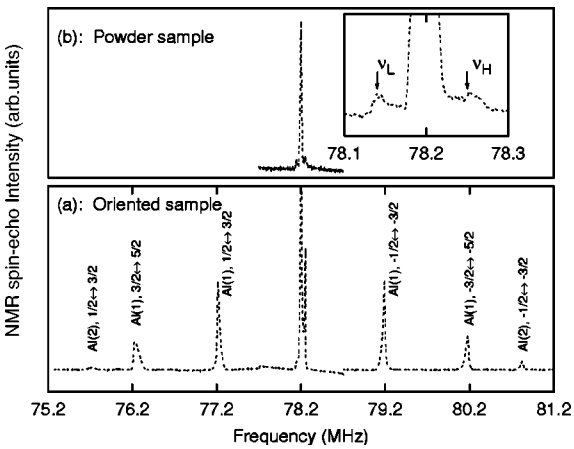

FIG. 5. ^{27}Al NMR spectra of $LaNi_2Al_5$ in the partially oriented powder (a), and randomly oriented powder (b) at 7.04 T at 300 K. The inset in (b) shows the central part in the expanded scale. The typical powder pattern relevant to the second-order quadrupole interaction for the Al(2) site is evident by prominent points ν_H and ν_L as described in the text.

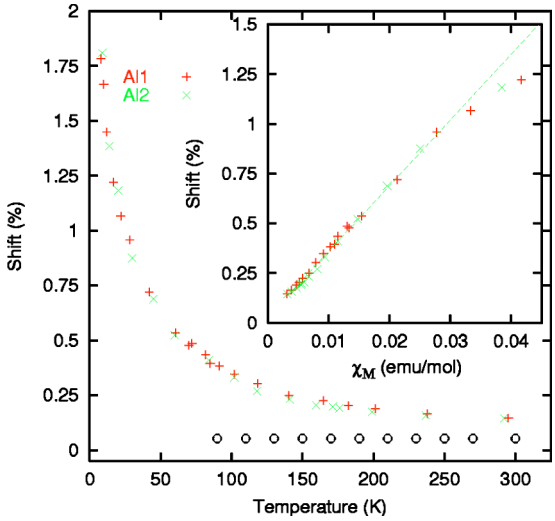

FIG. 6. (Color online) Variation of the Knight shift, K% with T in +, ×: $CeNi_2Al_5$ and ○: $LaNi_2Al_5$. The inset shows the variation of K% with χ_M along the b axis.

order quadrupolar split central transition[16] belonging to the Al(2) site. A rough estimation of ν_Q from $\nu_H - \nu_L = \frac{25}{144}\left[I(I+1) - \frac{3}{4}\right](\nu_Q^2/\nu_R)$ gives a value close to that derived from the data measured in the oriented sample.

C. Shift and the hyperfine field

The temperature dependence of the Knight shift (K) is shown in Fig. 6. It is seen that K increases continuously with the lowering of temperature down to 3.5 K. The inset of Fig. 6 shows the variation of K with the bulk molar susceptibility, χ_M along the b axis. Since the susceptibility of the reference compound $LaNi_2Al_5$ is very small, the measured susceptibility of $CeNi_2Al_5$ can be identified as being due to the f-electron susceptibility, χ_M^f. K is found to vary linearly with χ_M in the range 30–300 K. As long as the contribution due to K_{an} is negligible, following Carter *et al.*,[17] the experimental Knight shift can be written as $K_{iso} = K_0 + K_{s\text{-}f}(T)$, which reduces to

$$K_{iso} = K_0 + (H_{hf}/N\mu_B)\chi_M^f(T), \tag{2}$$

where K_0 is the shift due to s-conduction electrons and $K_{s\text{-}f}(T)$ is due to s-f exchange interaction. H_{hf} is the transferred hyperfine field, N is Avogadro's number, and μ_B is Bohr magneton. A linear fit of this curve to Eq. (2) gives the values of K_0 and H_{hf} as 0.03% and 1.842 kOe/μ_B, respectively. The measured H_{hf} is small and close to that found in $CeNiAl_4$ (Ref. 6), but cannot be explained by the dipolar fields of the magnetic moments of the Ce-4f electrons.

It is to be noted that K_0 for $LaNi_2Al_5$ is found to be ~0.05%. Subtracting the value of K_0 from the measured K, the contribution to the shift due to s-f exchange interaction (K_f) is estimated. Figure 7 shows the linear variation of $1/K_f$ with temperature with an intercept at −8.5 K on the temperature axis. Though the value of the Curie-Weiss temperature (θ_P) along the three crystallographic axes is not mentioned in the single-crystal susceptibility results,[8] the nature of the $1/\chi$ versus temperature curves, indicate a small value of θ_P along the b axis, whereas the same for the a and c axes of the crystal are considerably larger in magnitude with a negative sign. Thus the value of θ_P determined from the present NMR data in oriented ($H \| b$) powder agrees quite well with that of the single-crystal susceptibility result.

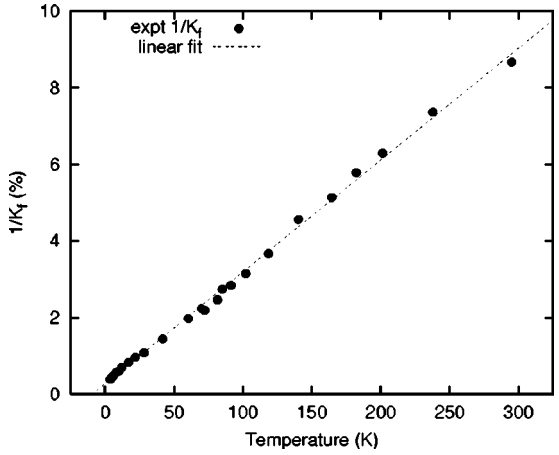

FIG. 7. Temperature dependence of the inverse of the Knight shift $1/K_f$ in $CeNi_2Al_5$.

IV. NUCLEAR SPIN-LATTICE RELAXATION

The magnetic spin-lattice relaxation of a nucleus with spin $I=5/2$ with quadrupole splitting of the nuclear Zeeman levels is governed by master equations[18] that predict a multiexponential behavior. In case of saturation recovery with a short saturation sequence, the recovery of the $m \leftrightarrow m-1$ transitions are as follows:

$1/2 \leftrightarrow -1/2$ transition:

$$\frac{M(\infty) - M(t)}{M(\infty)} = C\left[0.029\exp\left(\frac{-2t}{T_1}\right) + 0.178\exp\left(\frac{-6t}{T_1}\right) + 0.794\exp\left(\frac{-15t}{T_1}\right)\right];$$

$\pm 3/2 \leftrightarrow \pm 1/2$ transition:

$$\frac{M(\infty) - M(t)}{M(\infty)} = C\left[0.028\exp\left(\frac{-t}{T_1}\right) + 0.053\exp\left(\frac{-3t}{T_1}\right) + 0.025\exp\left(\frac{-6t}{T_1}\right) + 0.446\exp\left(\frac{-10t}{T_1}\right) + 0.446\exp\left(\frac{-15t}{T_1}\right)\right];$$

$\pm 5/2 \leftrightarrow \pm 3/2$ transition:

$$\frac{M(\infty) - M(t)}{M(\infty)} = C\left[0.028\exp\left(\frac{-t}{T_1}\right) + 0.214\exp\left(\frac{-3t}{T_1}\right) + 0.4\exp\left(\frac{-6t}{T_1}\right) + 0.286\exp\left(\frac{-10t}{T_1}\right) + 0.071\exp\left(\frac{-15t}{T_1}\right)\right].$$

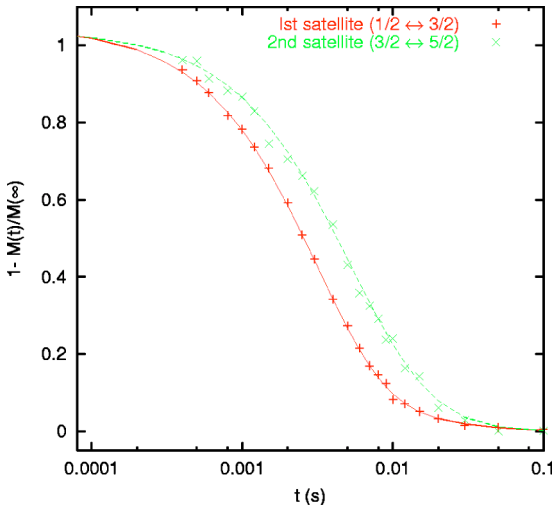

FIG. 8. (Color online) Nuclear magnetization recovery $1-M(t)/M(\infty)$ for ^{27}Al first and second satellite transitions for the Al(1) site in $CeNi_2Al_5$ at 300 K.

The constant C and the spin-lattice relaxation time T_1 are the two parameters to be determined by fitting the experimental recovery curves. As the central transitions of the Al(1) and Al(2) sites remain superimposed throughout the whole temperature range, the measurements of T_1 were performed using the satellite transitions that are well resolved, as mentioned in Sec. III. Thus by allowing selective stimulation of one of the satellites, by applying a single $\pi/2$ pulse, the growth of the solid echo was monitored at variable delays. Figure 8 shows the recovery curves for the two satellite transitions for the Al(1) site at 300 K. The values of T_1 obtained from the two transitions were found to agree quite satisfactorily. It is to be noted that in Fig. 8 the decay curve for $\pm\frac{1}{2}\leftrightarrow\pm\frac{3}{2}$ transition remains below that of $\pm\frac{3}{2}\leftrightarrow\pm\frac{5}{2}$ transitions. Such a decay behavior confirms the predominance of the magnetic relaxation over the quadrupolar one in the present system and justifies the use of equations for magnetic relaxation.[19] In this compound, $1/T_1$ is given by

$$1/T_1 = 1/T_{1K} + 1/T_{1f}, \tag{3}$$

where the first term represents the Korringa contribution due to contact interaction with conduction electrons

$$1/T_{1K} = \pi\hbar^3\gamma_e^2\gamma_n^2A_{hf}^2N(E_F)^2k_BT, \tag{4}$$

where A_{hf} is the transferred hyperfine coupling and $N(E_F)$ is the density of electronic states at the Fermi level. Hence for heavy fermion systems, $1/T_{1K}$ also provides access to the hybridization-enhanced density of states at the Fermi level. The second term, $1/T_{1f}$ arises due to the f-electron spin fluctuations that will be transferred via RKKY interactions from local moments to the site of the NMR nucleus and is given by[20]

$$1/T_{1f} = \gamma_N^2k_BT\sum_{\mathbf{q}}[H_{hf}(\mathbf{q})]^2\chi''(\mathbf{q},\omega_0)/\omega_0, \tag{5}$$

where $H_{hf}(\mathbf{q})$ is the spatial Fourier transform of the transferred hyperfine field $H_{hf}(r)$ between a Ce^{3+} ion and an Al nucleus separated by a distance r. $1/T_{1f}$ is therefore sensitive to correlation between the stochastic motions of Ce neighbors as well as to the single Ce spin-fluctuation time. A convenient definition of the latter quantity for NMR is given by[21]

$$\tau = \frac{\sum_q \chi''(\mathbf{q},\omega_0)/\omega_0}{N\chi'(0,0)}. \tag{6}$$

The summation is over the spatial fluctuation modes with wave vector $\mathbf{q}$. The frequency dependence of τ is very small if the nuclear resonance frequency ω_0 is much less than the characteristic fluctuation rates, i.e., if $\omega_0\tau\ll 1$. If the probe nuclei are each coupled to only one $4f$ ion, then it can be shown that[22]

$$\chi/K^2T_{1f}T = 2N\gamma_n^2k_B\tau, \tag{7}$$

where χ is the bulk $4f$ susceptibility. In the more general case, the above equation still holds,[22] with τ replaced by

$$\tau_{eff} = \frac{\left[\sum_{\mathbf{q}}|H_{hf}^{\mathbf{q}}|^2\chi''(\mathbf{q},\omega_0)/\omega_0\right]}{N[H_{hf}^0]^2\chi'(0,0)}. \tag{8}$$

If a given nucleus is coupled to only one magnetic ion, $H_{hf}^{\mathbf{q}}$ is independent of $\mathbf{q}$, and Eq. (8) reduces to Eq. (6).

If the local moment fluctuation frequency, ω_{fl} (τ^{-1}) is much faster than the nuclear Larmor frequency, then the expression for $1/T_{1f}$ may be expressed as[23]

$$1/T_{1f} \approx \gamma_n^2H_{hf}^2/\omega_{fl}. \tag{9}$$

In general, ω_{fl} is given by two major processes, i.e., ω_{ex} and ω_{cf}. The former is caused by exchange interactions among local moments and is given by $\omega_{ex}^2=8zJ_{ex}^2[J(J+1)]/(3\hbar^2)$. The latter is due to the spin-exchange interaction with conduction electrons given by $\omega_{cf}=\pi\hbar[J_{cf}N(E_F)]^2k_BT$. Here, J_{ex} is the superexchange coupling between Ce moments, and J_{cf} is the spin-exchange coupling between the Ce local moments and conduction electrons. It is to be noted that the former predicts a temperature-independent T_1, while the latter gives a T-dependent T_1 process.

Figure 9 shows the variation of $1/T_1$ with temperature for Al(1) and Al(2) sites in $CeNi_2Al_5$ along with those in $LaNi_2Al_5$. Interestingly it may be seen that in $CeNi_2Al_5$, the nature and the magnitude of $1/T_1$ are different for the two Al sites throughout the temperature range 3.5–300 K, though there is no measurable difference in the Knight shift (Fig. 6). On the other hand, in the La compound [where only the contribution T_{1K} is present with $(T_1T)^{-1}=0.025$ (s K^{-1})] the values of T_1 for the two sites are found to be same throughout the range 80–300 K. This finding suggests that the difference in $1/T_1$ for the two Al sites in case $CeNi_2Al_5$ arises due the difference in the fluctuating part of the magnetic field produced by the Ce-$4f$ electron, whereas the time-averaged part of the fluctuating magnetic field, produced by the same Ce-$4f$ electron at the Al nuclear sites resulting in the shift of the resonance lines, are same for both the sites. Thus the long wavelength $(\mathbf{q}=0)$ part of the dynamic spin susceptibility contributing to the Knight shift is same for the two Al sites

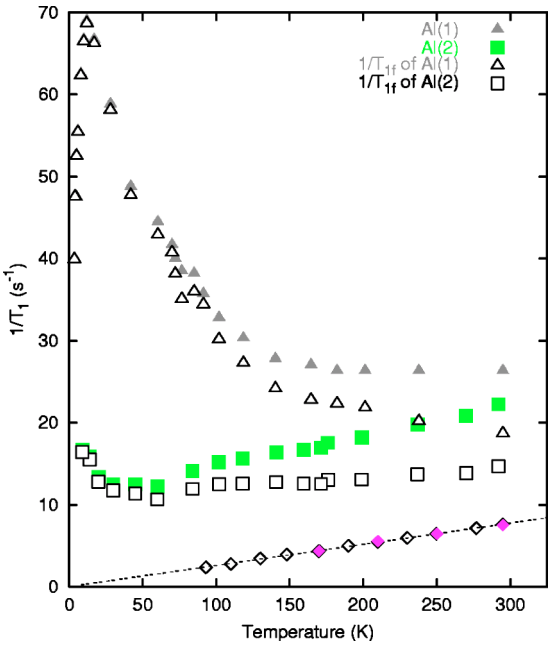

FIG. 9. (Color online) Temperature dependence of the ^{27}Al spin-lattice relaxation rate for the ▲: Al(1), ■: Al(2) sites of $CeNi_2Al_5$, respectively, and ◇: Al(1) and ◆: Al(2) sites of $LaNi_2Al_5$. △: $1/T_{1f}$ for Al(1) and □: $1/T_{1f}$ for Al(2), obtained after subtracting the $1/T_{1K}$ contribution for $LaNi_2Al_5$ from experimental $1/T_1$ values of $CeNi_2Al_5$.

and changes equally with temperature. The contribution due to the short wavelength components affecting the Al nuclear relaxation process for the two Al sites, are different both in nature and magnitude throughout the whole temperature range.

In order to understand this result, it is necessary to determine the temperature dependence of $1/T_{1f}$ for the two Al sites. For this the Korringa contribution $1/T_{1K}$, determined in $LaNi_2Al_5$, has been subtracted from the measured values of $1/T_1$ of $CeNi_2Al_5$. The variation of $1/T_{1f}$ with temperature is also shown in Fig. 9 by open triangles and open squares for Al(1) and Al(2), respectively. In the range 150–300 K, $1/T_{1f}$ for Al(1) increases slowly with the lowering of temperature, indicating a dominant contribution of ω_{cf} in ω_{fl} in Eq. (9). The rate of increment of $1/T_1$ then is enhanced appreciably below 150 K, suggesting the development of short-range magnetic correlations between the Ce-4f electron moments. Below 12 K, $1/T_{1f}$ decreases sharply down to 3.5 K, indicating the effect of the slowing down of the Ce-4f electron spin-fluctuation rate. The peak thus appears at a temperature (12 K) that is much higher than the reported T_N = 2.6 K. A similar shift in the peak position of $1/T_{1f}$ from T_N, by about 7 K towards the high-temperature side was also observed in the case of $CeAl_2$ from ^{27}Al NQR studies.[21] Thus the shift in the peak position from T_N as observed in the case of $CeNi_2Al_5$ could not be attributed to the effect of the external magnetic field. Nevertheless, the appearance of this maximum near the magnetic phase transition, may be attributed to critical fluctuation on the time scale corresponding to the Larmor frequency of the ^{27}Al nucleus.

For the Al(2) site in the range 12–300 K, $1/T_{1f}$ is almost temperature independent according to Eq. (9), as if this site

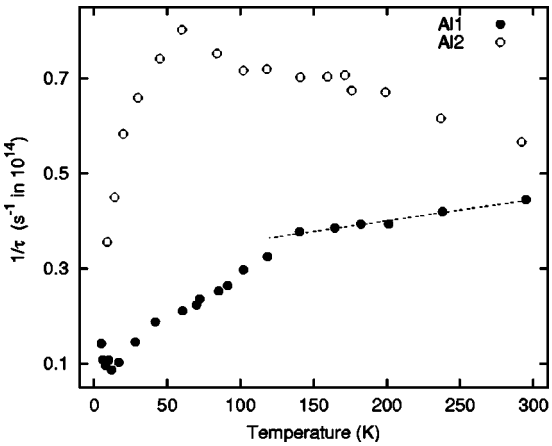

FIG. 10. Temperature dependence of the fluctuation rates $1/\tau$ in $CeNi_2Al_5$ as estimated from Eq. (7) using the data for the Al(1) and Al(2) sites.

is experiencing a fluctuating magnetic field from the Ce-4f electrons whose time scale is much faster than the Larmor frequency, ω_0. As the resonance positions for the Al(1) and Al(2) sites are coincident in the whole temperature range 3.5–300 K, they have the same value of ω_0. Thus it seems that the Al(2) site is not experiencing the effect of development of short-range magnetic correlations in the range 12–300 K, whereas Al(1) is sensing the same below 150 K. However, it starts to sense this effect below 12 K resulting in an enhancement of $1/T_{1f}$ without showing any peak down to 3.5 K. The almost temperature-independent behavior of $1/T_{1f}$ in case of the Al(2) site over the range 12–300 K suggests the dominance of the ω_{ex} term in $1/T_{1f}$, with $\omega_{ex} \gg \omega_0$. Moreover the magnitude of $1/T_{1f}$ in the measured $1/T_1$ of the Al(2) site is less compared to the Korringa part, so that over a wide temperature range of 12–300 K, the Korringa behavior dominates in the temperature dependence of $1/T_1$ for the Al(2) site and therefore is almost parallel to that of the $1/T_1$ vs T curve of $LaNi_2Al_5$. This finding suggests that for the Al(2) site, the effect of the 4f spin fluctuations due to the Kondo effect dominates over that of the RKKY interaction. The result also indicates that the correlated spin fluctuations of the Ce ions close to the Al(2) site start to develop at a much lower temperature (12 K). It could be due to the stronger Kondo effect over the RKKY interaction around the Al(2) site as if the $s-f$ hybridization around this site is greater than that around the Al(1) site. These widely different mechanisms in the nuclear spin-lattice relaxation processes of two inequivalent Al sites over a large temperature range is a rather strange observation in a dense Kondo system that exhibits magnetic ordering.

Figure 10 shows the temperature dependence of $1/\tau$ for the two Al sites determined from the present NMR data, using Eq. (7). It is seen that for the Al(1) site, $1/\tau \propto T$ in the range 150–300 K. This suggests that in this temperature range the 4f local moments are noninteracting and are relaxed via Korringa-type scattering with the conduction electrons. This finding further supports the behavior of $1/T_{1f}$ vs T curve for Al(1). In the Korringa limit, the expression for $1/\tau$ is given by

$$1/\tau = 8\pi^2 k_B T(JN(E_F))^2/h, \quad (10)$$

where J is the $s-f$ exchange integral. The value of $JN(E_F)$ determined from the slope of the dotted line (Fig. 10) is 0.166, suggesting a low carrier density. However, below 150 K, $1/\tau$ decreases continuously down to 12 K, where $1/T_{1f}$ again shows an increasing trend. This finding indicates the possibility of the development of Ce-4f spin correlations at finite q below 150 K. Below 12 K, $1/\tau$ again shows an increasing trend down to 3.5 K. On the other hand, in the case of the Al(2) site, $1/\tau$ increases continuously in the range 60–300 K, which could be a signature of the gradual enhancement of the 4f spin fluctuation due to the Kondo effect resulting in the dominance of the Korringa contribution to the Al nuclear relaxation process over that due to the RKKY interaction. Below this range it decreases sharply down to 3.5 K, which may be the result of the development of **q**-dependent 4f-spin correlations from below 60 K, around the Al(2) site. However, the effect of the development of such correlations are observed in the behavior of $1/T_{1f}$ of the Al(2) nuclear site, from the much lower temperature of ~12 K.

One must also consider, in rare-earth metals, the effect of CEF in the 4f moment. In $CeNi_2Al_5$, it is very large[8] and the first excited state is situated 200 K above the ground state of the Kramers' doublets. Therefore, the behavior of $1/\tau$, experienced by the Al(1) site below 150 K may also be influenced by the CEF effect beside the **q**-dependent contribution of the dynamic susceptibility. But we have to rule out the CEF effect in the deviation of $1/\tau$ below ~60 K experienced by the Al(2) site as seen in Fig. 10.

Finally, it is to be noted that the T dependence of $1/T_1$ in $CeNi_2Al_5$ differs appreciably from that of other Ce-based compounds.[5,6,24] We will take the case of $CeNiAl_4$ in a little more detail, as the Ce environment is rather similar for $CeNiAl_4$ (13 Al and 4 Ni; site symmetry $mm2$) and $CeNi_2Al_5$ (14 Al and 4 Ni; site symmetry mmm).[2] In $CeNiAl_4$, above 20 K, the Korringa term dominates in $1/T_1$ for all Al sites, together with the temperature-independent contribution due to the Ce-4f spin fluctuation ($\omega_{fl} \gg \omega_0$).[6] In the range 3.8–20 K, however, $1/T_{1f}$ decreases, indicating the appearance of 4f spin compensation.

V. CONCLUSION

We have presented the results of ^{27}Al NMR study in grain-aligned $CeNi_2Al_5$. The temperature dependence of the Knight shift and $1/T_1$ were measured in the range 3.5–300 K for two inequivalent aluminum sites present in the unit cell. For comparison, ^{27}Al NMR results of partially aligned $LaNi_2Al_5$ in the range 80–300 K have also been included. In the latter, the Knight shift is temperature independent and $1/T_1$ follows the Korringa relation normal to nonmagnetic intermetallics. Moreover, quadrupolar interaction parameters for these two compounds are very close to each other confirming the isomorphous structure. Ce-4f electronic contribution to the hyperfine field and $1/T_1$ in $CeNi_2Al_5$ have been derived after subtracting the relevant contribution obtained for $LaNi_2Al_5$.

We summarize the results of $CeNi_2Al_5$ as follows: (1) The Knight shift of the two inequivalent Al sites behave identically throughout the range 3.5–300 K. The value of θ_P estimated from shift data agrees well with that of single-crystal susceptibility data. (2) The behavior of $1/T_{1f}$ for the two Al sites are widely different. For the Al(1) site, with one nearest-neighbor Ce ion, the 4f electron-spin-fluctuation process dominates over the Korringa contribution throughout the temperature range studied. In particular, the Ce-4f spin correlation nearest to Al(1) starts to develop below 150 K. Finally, near 12 K, the fluctuation frequency of the 4f spin becomes comparable to the ^{27}Al NMR frequency resulting in the reduction of $1/T_{1f}$ with further lowering of the temperature. (3) For the Al(2) site, which sits in between two Ce near neighbors, the relaxation process is dominated by the Korringa contribution in the range 12–300 K. It could, however, sense the effect of the development of the Ce-4f spin correlations, below 12 K, with a small enhancement of $1/T_{1f}$, from where the same for the Al(1) site starts to reduce. (4) The widely different ^{27}Al nuclear relaxation mechanisms for two inequivalent Al sites in the unit cell of $CeNi_2Al_5$ is a strange observation. It seems that the effect of spin fluctuation due to the Kondo effect overcomes that due to the RKKY interaction for the Al(2) site in the range 12–300 K. On the other hand, the behavior of $1/T_{1f}$ for the Al(1) site resembles to that of $CeAl_2$, which also exhibits an antiferromagnetic ordering with T_N=3.9 K (Ref. 21), similar to $CeNi_2Al_5$, which has T_N=2.6 K.

ACKNOWLEDGMENTS

R.S. is grateful to CSIR, India for providing him financial assistance by awarding JRF(NET) [F. No. 2-48/2001(II)EU.II]. We are thankful to D. J. Seth and B. Pahari for their help in the experiment.

*Electronic address: agr@cmp.saha.ernet.in

[1] O. Zarechnyuk, T. I. Yanson, and R. M. Rykhal, Izv. Akad. Nauk. SSSR, Met. **4**, 192 (1983).

[2] D. Gout, E. Benbow, O. Gourdon, and G. J. Miller, J. Solid State Chem. **176**, 538 (2003).

[3] T. Mizushima, Y. Ishikawa, A. Maeda, K. Oyabe, K. Mori, K. Sato, and K. Kamigaki, J. Phys. Soc. Jpn. **60**, 753 (1991).

[4] T. Mizushima, Y. Ishikawa, K. Oyabe, K. Mori, and J. Sakurai, Physica B **186**, 457 (1993).

[5] K. Ghoshray, B. Bandyopadhyay, and A. Ghoshray, Phys. Rev. B **65**, 174412 (2002).

[6] K. Ghoshray, B. Bandyopadhyay, and A. Ghoshray, J. Magn. Magn. Mater. **272-276**, 32 (2004).

[7] Y. Isikawa, T. Mizushima, K. Oyabe, K. Mori, K. Sato, and K.

Kamigaki, J. Phys. Soc. Jpn. **60**, 1869 (1991).
[8] Y. Isikawa, T. Mizushima, J. Sakurai, K. Mori, A. Munoz, F. Givord, J. Boucherle, J. Voiron, S. Oliviera, and J. Flouquet, J. Phys. Soc. Jpn. **63**, 2349 (1994).
[9] F. Givord, J.-X. Boucherle, J. Dreyer, Y. Isikawa, B. Ouladdiaf, S. Pujol, J. Schweizer, and F. Tasset, J. Phys.: Condens. Matter **11**, 7327 (1999).
[10] Y. Ishikawa, S. Aklamaru, T. Mizushima, T. Kuwai, J. Sakurai, K. Tenya, T. Takikawa, T. Sakakibara, T. Takeuchi, and Y. Miyako, J. Magn. Magn. Mater. **226-230**, 205 (2001).
[11] K. Fujiwara, Y. Yamanashi, and K. Kumagai, Physica B **186-188**, 599 (1993).
[12] K. Maezawa, S. Akamaru, T. Kuwai, Y. Ishikawa, J. Sakurai, and H. Harima, J. Phys. Soc. Jpn. **68**, 2697 (1999).
[13] Y. Ishikawa, H. Takagi, A. Ishiguro, M. Yasumoto, T. Kuwai, T. Mizushima, J. Sakurai, A. Sawada, T. Komatsubara, K. Maezawa, and H. Harima, J. Phys. Soc. Jpn. **68**, 2802 (1999).
[14] J. Rodríguez-Carvajal, Physica B **192**, 55 (1993).
[15] K. Ghoshray, B. Bandyopadhyay, and A. Ghoshray, Phys. Rev. B **69**, 094427 (2004).
[16] A. Abragam, *The Principles of Nuclear Magnetism* (Clarendon, Oxford, 1961).
[17] C. Carter, L. H. Bennett, and D. J. Khan, Prog. Mater. Sci. **20**, 1 (1977).
[18] E. R. Andrew and D. P. Tunstall, Proc. Phys. Soc. London **78**, 1 (1961).
[19] W. W. Simmons, W. J. O'Sullivan, and W. A. Robinson, Phys. Rev. **127**, 1168 (1962).
[20] C. H. Pennington and C. P. Slichter, *Physical Properties of High Temperature Superconductors* (World Scientific, Singapore, 1990), Vol. II.
[21] D. E. MacLaughlin, O. Pena, and M. Lysak, Phys. Rev. B **23**, 1039 (1981).
[22] D. E. MacLaughlin, F. R. de Boer, J. Bijvoet, P. de Châtel, and W. C. M. Mattens, J. Appl. Phys. **50**, 2094 (1979).
[23] T. Moriya, Prog. Theor. Phys. **16**, 23 (1956).
[24] P. Vonlanthen, J. Gavilano, B. Ambrosini, and H. R. Ott, Eur. Phys. J. B **7**, 9 (1999).